PPS
Paper
www.rsc.org/pps

# Photoreduction of bicarbonate catalyzed by supported cadmium sulfide †

**Horst Kisch* and Peter Lutz**

*Institut für Anorganische Chemie, Universität Erlangen-Nürnberg Egerlandstraße 1, D-91058 Erlangen, Germany*

***Received 4th December 2001, Accepted 30th January 2002***
***First published as an Advance Article on the web 11th February 2002***

Cadmium sulfide supported on silica (CdS-*x*/$SiO_2$, $x = 4$, 11, 17, 25%) and zinc sulfide (CdS-*x*/ZnS, $x = 5$, 10, 20, 30%) was prepared by impregnation with cadmium sulfate and subsequent addition of sodium sulfide. The specific surface areas of the silica and zinc sulfide supported powders are in the range of 188–280 and 95–104 $m^2\ g^{-1}$, respectively. After sonication of an aqueous suspension of CdS-17/$SiO_2$ the particle size distribution exhibited two maxima at 22 and 57 μm. In the presence of sodium sulfite the supported cadmium sulfides photocatalyze the reduction of bicarbonate to formate, formaldehyde, and oxalate. Upon polychromatic irradiation ($\lambda \geq 290$ nm) the $C_1$-products formate and formaldehyde were obtained in concentrations of 30–130 μM whereas the $C_2$-product oxalate reached only 1–8 μM. Formaldehyde is not formed through reduction of intermediate formate whereas oxalate is produced *via* oxidation of the latter. The linear increase of oxalate concentration with coverage can be rationalized by the assumption that dimerization of the intermediate carbon dioxide radical anion does not occur on the cadmium sulfide but in solution or on the silica surface. For zinc sulfide supported samples the coverages of 10, 20, and 30% do not change the photocatalytic activity significantly whereas a loading of 5% induces a 40-fold and 16-fold increase as compared to unmodified cadmium and zinc sulfide, respectively. This strong enhancement suggests that in CdS-05/ZnS the efficiency of charge separation is strongly improved through interparticle electron transfer. The results demonstrate that both silica and zinc sulfide supports increase the photocatalytic activity of cadmium sulfide through the presence of a recently found electronic semiconductor-support interaction (SEMSI effect). Additionally, the low coverage sample CdS-05/ZnS combines this novel effect with the higher charge separation efficiency of a coupled semiconductor system.

## Introduction

The quantum yield of a semiconductor catalyzed photoreaction is largely determined by three factors. By the efficiency of the photoinduced formation of reactive electrons and holes ($e_r^-$, $h_r^+$), the efficiency of interfacial electron transfer to and from dissolved substrates (IFET), and the efficiency by which the primary electron transfer intermediates are transformed to the final products. For a given semiconductor–substrate system the first two factors in particular may be strongly influenced by minor modifications of the semiconductor. One way to increase the efficiency of charge separation, and therefore the first factor, is to couple the semiconductor in question to a second one having appropriate energy levels.[1] A possibility for increasing the importance of the second factor is to support the semiconductor on a photoinactive material like silica which is thought to improve substrate adsorption and therefore increase the efficiency of the IFET.[2] The third factor is dominated primarily by the reactivity of intermediate radicals and radical ions and therefore much less modifiable for a given reaction. Photofixation of carbon dioxide with visible light is of primordial importance both in relation to fundamental and practical aspects. It is known that CdS, as colloid or powder, may induce photoreduction[3] and C–C coupling reactions.[4] In general the product yields are in the order of micromoles and photocorrosion is often the limiting factor. Recently we have found that CdS supported on silica at the fixed coverage of 40% is a superior photocatalyst compared to the unsupported sulfide and does not suffer photocorrosion.[5] In the following we report on the influence of varying the coverage of silica and changing the support from photoinactive silica to photoactive zinc sulfide. These modifications are expected to influence the two first efficiency factors and therefore also the quantum yield. In all reactions sodium bicarbonate was employed as carbon dioxide equivalent and sodium sulfite as reducing agent. In addition to formate and formaldehyde, oxalate was also observed as reduction product (Fig. 1).

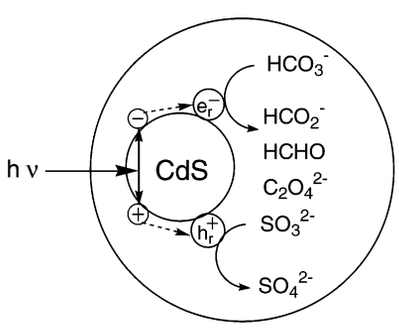


**Fig. 1** Schematic reactions of bicarbonate photoreduction at supported CdS. The inner and outer circle represent a cadmium sulfide and $SiO_2$ or ZnS particle, respectively.

## Experimental

### Analytical methods

HPLC: Knauer 64 instrument, Eurokat-H column (300 × 8 mm) type 146, 0.025 M $H_2SO_4$ as eluting agent (0.4 mL $min^{-1}$), UV-Vis filter photometer for detection ($\lambda \geq 200$ nm),

† Dedicated to Professor Gottfried Huttner on the occasion of his 65th birthday.

 DOI: 10.1039/b111092f

250 μL injected sample volume. Ion chromatography: Dionex Quick Analyzer, 1.7 mmol $L^{-1}$ of $NaHCO_3$–1.8 mmol $L^{-1}$ of $Na_2CO_3$ as eluting agent, 1 mL of conc. $H_2SO_4$ in 2 L of $H_2O$ for regeneration, conductivity detector, 1 mL injected sample volume. Specific surface area: through $N_2$-adsorption according to the Brunnauer–Emmet–Teller method. Elemental analysis: CARLO ERBA Elemental Analyzer Model 1108. Particle size distribution: laser diffractometer (Retsch). Intensity measurement: Radiant Power/Energy Meter Model 70260 (Oriel Instruments). Product analysis: formate and oxalate were determined by HPLC and ion chromatography, formaldehyde was determined colorimetrically[6] in samples drawn through a Millipore membrane filter (0.22 μm pores) from the reacting suspension under dinitrogen. Error bars given in Fig. 3 and 4 indicate reproducibility. All reported values are the average of 2 or 3 experiments.

### Materials

CdS and ZnS of specific surface areas of 142 and 94 $m^2\ g^{-1}$, respectively, were prepared as described.[7,8] $SiO_2$ (Grace 432, 340 $m^2\ g^{-1}$) was used as obtained.

CdS-*x*/$SiO_2$: 10 g of $SiO_2$ were stirred for 24 h with the corresponding amount of cadmium sulfate dissolved in 150 mL of 10% ammonia solution. Thereafter 100 mL of an equimolar sodium sulfide solution was added dropwise. After filtration the yellow powder was dried over Siccapent in a desiccator, ground in a mortar, and stored under dinitrogen.

CdS-04/$SiO_2$: $S_{calcd}$ 1.25%, $S_{found}$ 0.93%. Atomic absorption spectroscopy (AAS): $Cd_{calcd}$ 4.4%, $Cd_{found}$ 2.8%; 280 $m^2\ g^{-1}$.

CdS-11/$SiO_2$: $S_{calcd}$ 2.37%, $S_{found}$ 2.35%. AAS: $Cd_{calcd}$ 8.3%, $Cd_{found}$ 7.0%; 250 $m^2\ g^{-1}$.

CdS-17/$SiO_2$: $S_{calcd}$ 5.10%, $S_{found}$ 3.80%. AAS: $Cd_{calcd}$ 17.9%, $Cd_{found}$ 12.4%; 233 $m^2\ g^{-1}$.

CdS-25/$SiO_2$: $S_{calcd}$ 6.35%, $S_{found}$ 5.60%. AAS: $Cd_{calcd}$ 22.2%, $Cd_{found}$ 17.5%; 188 $m^2\ g^{-1}$.

CdS-*x*/ZnS: 2 g of ZnS were treated with the corresponding cadmium sulfate solution as described for $SiO_2$. Thereafter 50 mL of the equimolar sodium sulfide solution was added dropwise.

CdS-05/ZnS: $S_{calcd}$ 32.4%, $S_{found}$ 31.06%. AAS: $Cd_{calcd}$ 3.9%, $Cd_{found}$ 3.9%; $Zn_{calcd}$ 63.7%, $Zn_{found}$ 61.6%; 95 $m^2\ g^{-1}$.

CdS-10/ZnS: $S_{calcd}$ 31.9%, $S_{found}$ 30.85%. AAS: $Cd_{calcd}$ 7.8%, $Cd_{found}$ 7.4%; $Zn_{calcd}$ 60.3%, $Zn_{found}$ 57%; 97 $m^2\ g^{-1}$.

CdS-20/ZnS: $S_{calcd}$ 30.73%, $S_{found}$ 29.76%. AAS: $Cd_{calcd}$ 15.6%, $Cd_{found}$ 16.0%; $Zn_{calcd}$ 53.6%, $Zn_{found.}$ 52.3%; 101 $m^2\ g^{-1}$.

CdS-30/ZnS: $S_{calcd}$ 30.73%, $S_{found}$ 29.76%. AAS: $Cd_{calcd}$ 17.9%, $Cd_{found}$ 18.2%; $Zn_{calcd}$ 51.6%, $Zn_{found}$ 49.7%; 104 $m^2\ g^{-1}$.

### Irradiations

Two irradiation set-ups were employed. A merry-go-round apparatus allowed simultaneous irradiation (water cooled Osram 100 W tungsten halogen lamp) of suspensions contained in 9 water cooled test tubes (10 mL volume, pyrex glass) under continuous magnetic stirring. The second apparatus consisted of an optical train equipped with a cylindrical, water-cooled 15 mL quartz cuvette, a water filter, an Osram XBO 150 W xenon lamp contained in a light-condensing lamp housing (PTI A1010S). For selective excitation cut-off ($\lambda \geq 320$, 400 and 454 nm) and interference filters ($\lambda$ = 316 and 436 ± 5 nm) were placed in the light path. All experiments, including sample withdrawal, were performed under dinitrogen and the suspension was sonicated for 15 min prior to irradiation.

### Influence of support

Merry-go-round apparatus ($\lambda \geq 290$ nm); 10 mL of corresponding suspension prepared from 10 mg of CdS-17/$SiO_2$ and CdS-30/ZnS (1 g $L^{-1}$) and 0.033 M $NaHCO_3$ containing 0.005 M $Na_2SO_3$ were irradiated for 6 h (standard procedure). Formate was analyzed by HPLC. The color of CdS-30/ZnS did not change during irradiation whereas that of CdS-17/$SiO_2$ turned gray indicating $Cd^0$ formation.

**CdS-*x*/$SiO_2$.** *(a) Influence of coverage.* Standard procedure; formate, formaldehyde, and oxalate were detected as products.

*(b) Influence of catalyst concentration.* CdS-17/$SiO_2$ was employed in concentrations of 0.5, 1.0, 2.0, 3.0, 4.0 and 5.0 g $L^{-1}$ under standard conditions.

*(b) Influence of $HCO_3^-$ concentration on formate formation.* Standard procedure except that 20 mg of CdS-17/$SiO_2$ were suspended in 0.01, 0.02, 0.033, 0.04, and 0.06 M bicarbonate.

*(c) pH influence on formate formation.* Standard procedure except that 30 mg of CdS-17/$SiO_2$ were employed. Prior to sonication the pH value was adjusted to 5.3, 6.1, 10.0 and 11.9 by addition of HCl or NaOH. Photocorrosion occurred only at pH 6.1 as indicated by development of a gray color.

**CdS-*x*/ZnS.** Standard procedure except that the irradiation of 15 mL suspensions of CdS-05/ZnS, CdS-10/ZnS, and CdS-30/ZnS was performed on the optical train apparatus ($\lambda \geq 320$, 400, 455 nm). For comparison unsupported ZnS was also employed.

*(a) Monochromatic irradiations.* Standard procedure except that the optical train was used and an interference filter was placed in the light path. Intensities as measured with the radiometer were 27 μW $cm^{-2}$ at $\lambda$ = 436 nm and 0.76 μW $cm^{-2}$ at 316 nm. The unexpected higher intensity at the long wavelength is due to the higher transmittance of this filter; $\lambda$ = 316 ± 8 nm: UV.Pil Nr.60085.08 (Schott), $T_{max}$ 25%. $\lambda$ = 436 ± 10 nm: P/N 436FS10-50 AM-40187-1 (Andover), $T_{max}$ 35%.

*(b) Influence of sulfite concentration.* Standard procedure except that 48 mg of CdS-05/ZnS were suspended in 0.005 and 0.01 M $Na_2SO_3$. During 4 h of irradiation on the optical train samples were withdrawn every hour and analyzed for formate and sulfite.

*(c) Oxalate formation.* Standard procedure (merry-go-round) except that 30 mg of CdS-17/$SiO_2$ (3 g $L^{-1}$) suspended in a solution containing $HCO_2Na$ (0.004 M), $Na_2SO_3$ (0.005 M), and $NaHCO_3$ (0.033 M). No oxalate was detectable after 3 h of irradiation. When sulfite was omitted in the experiment described above, small amounts of oxalate were observable. When also $NaHCO_3$ was omitted (when 48 mg CdS-05/ZnS and 1 M $HCO_2Na$ were employed), oxalate amounts were much higher and correlated with decrease of formate concentration.

*(d) Formaldehyde formation.* Standard procedure using 10 mg of CdS-17/$SiO_2$ but replacing bicarbonate by 0.005 M $HCO_2Na$. Only disappearance of formate but no formaldehyde formation could be observed.

## Results

### Synthesis and characterization of supported photocatalysts

Supported CdS-*x*/$SiO_2$ and CdS-*x*/ZnS were prepared by impregnating $SiO_2$ or ZnS with a solution of cadmium sulfate and subsequent addition of sodium sulfide. Coverages (*x* = wt%) as determined from elemental analysis and atomic absorption spectroscopy were in the range of 4–30%, corresponding to 1–10 micromole of CdS per gram of support. After removing adsorbed gases at 200 °C, the specific surface area was measured through $N_2$ adsorption. Values of 188–280 and 95–104 $m^2\ g^{-1}$ were determined for the $SiO_2$ and ZnS supported samples, respectively (Table 1).

Determination of the particle size distribution by laser diffraction of aqueous suspensions revealed one maximum at 57 μm before and two maxima at 22 and 57 μm after sonication (Fig. 2).

**Table 1** Specific surface areas of $SiO_2$ and ZnS supported cadmium sulfides

| | Specific surface area/$m^2\ g^{-1}$ |
|---|---|
| CdS-04/$SiSO_2$ | 280 |
| CdS-11/$SiSO_2$ | 250 |
| CdS-17/$SiSO_2$ | 233 |
| CdS-25/$SiSO_2$ | 188 |
| CdS-05/ZnS | 95 |
| CdS-10/ZnS | 97 |
| CdS-20/ZnS | 101 |
| CdS-30/ZnS | 104 |

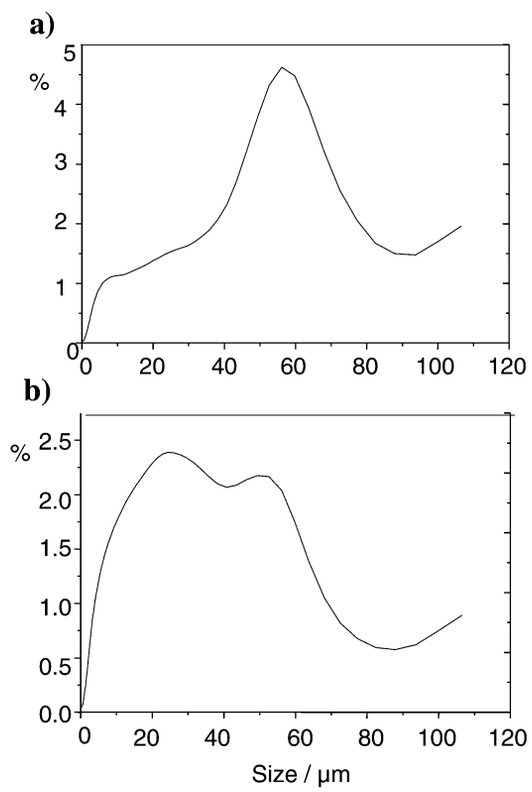


**Fig. 2** Particle size distribution of CdS-17/$SiO_2$ before (a) and after (b) sonication in water.

### Influence of support on photocatalytic activity

As displayed in Fig. 3 the amount of formate produced in presence of the supported and unsupported sample does not change significantly. However, since the total amount of CdS present differs considerably in these experiments, it is more appropriate to correct for this by dividing the product concentration through the amount of CdS present ("apparent turnover number" $TON_{app}$). From Fig. 3 it follows that this value increases by a factor of about six in the case of silica supported CdS. No corresponding number can be given for the ZnS supported sample since the support itself is photoactive under the experimental conditions.[5]

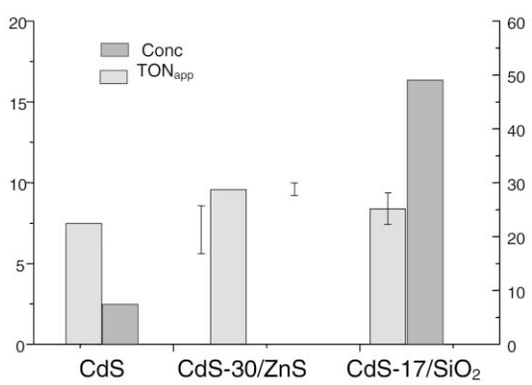


**Fig. 3** Absolute and per gram of CdS ($TON_{app}$) formate concentrations produced at 6 h of irradiation at $\lambda \geq 290$ nm.

### CdS-*x*/$SiO_2$

**Influence of coverage.** From Fig. 4 it follows that increasing the coverage has no signifcant influence on formate formation but induces a linear decrease in formaldehyde and a linear increase in oxalate concentrations. In the same direction $TON_{app}$ decreases much more strongly for formate and formaldehyde than for oxalate.

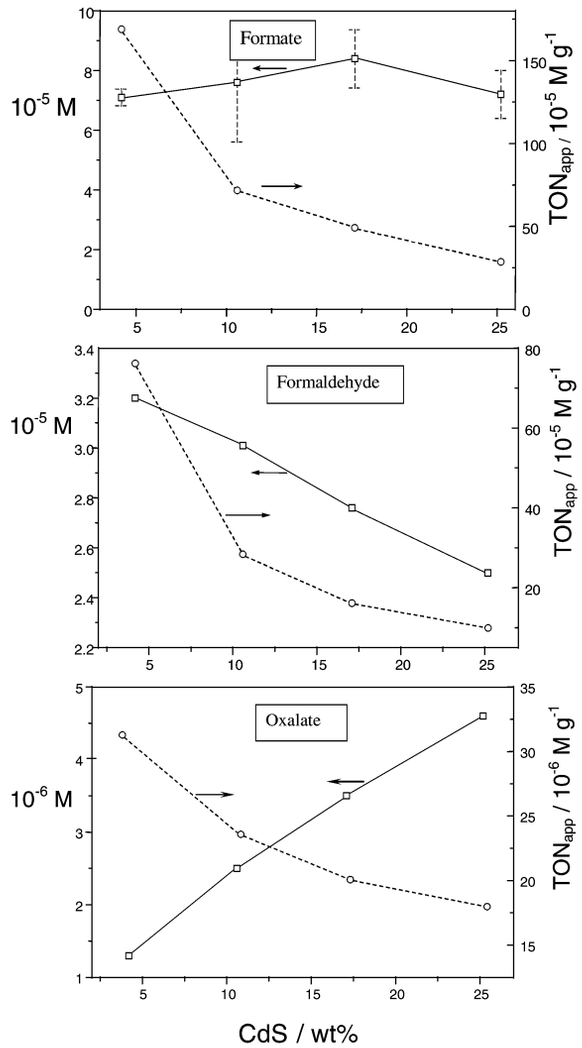


**Fig. 4** Product concentration and apparent turnover number ($TON_{app}$) as function of $SiO_2$ coverage; $\lambda \geq 290$ nm, 6 h.

**Influence of photocatalyst concentration.** For formate a maximum concentration is reached at the standard catalyst concentration of 1 g $L^{-1}$ whereas for formaldehyde and oxalate the corresponding value is twice as high (Fig. 5).

### CdS-*x*/ZnS

The first experiments were carried out at $\lambda \geq 455$ nm to prevent light absorption by the support (Fig. 6). Formate concentrations were in the range of 23 to 41 μM whereas under identical experimental conditions unsupported CdS afforded only traces of formate. When irradiation was conducted at $\lambda \geq 320$ nm in order that ZnS also could absorb light, formate concentrations rose with decreasing coverage from 40 to 80 up to 800 μM.

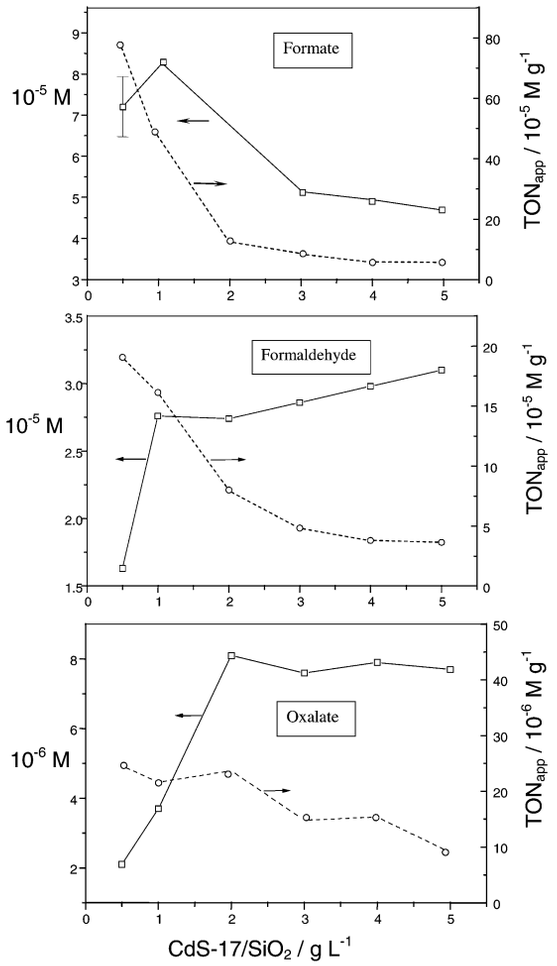


**Fig. 5** Product concentration and $TON_{app}$ as function of CdS-17/$SiO_2$ concentration; $\lambda \geq 290$ nm, 6 h.

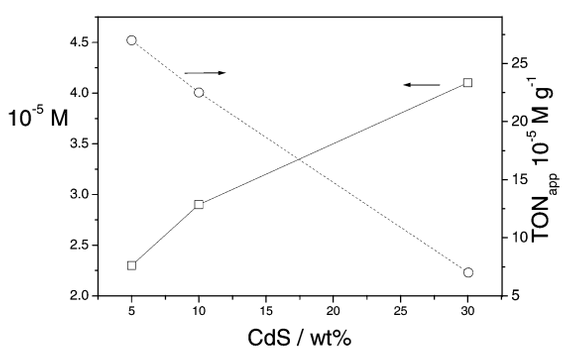


**Fig. 6** Formate concentration and $TON_{app}$ as function of ZnS coverage; $\lambda \geq 455$ nm, 3 h.

When in the system CdS-05/ZnS/$Na_2SO_3$ sulfite was replaced by 0.005 M sodium sulfide or sodium thiosulfate the initial rate of formate formation decreased from 0.16 μM $s^{-1}$ to 0.01 or 0.02 μM $s^{-1}$.

## Discussion

The specific surface areas of supported cadmium sulfides are governed by the component having the larger surface. In the case of CdS-*x*/$SiO_2$ this is the support $SiO_2$ (340 $m^2$ $g^{-1}$), in the case of CdS-*x*/ZnS, however, it is the photocatalyst CdS (142 $m^2$ $g^{-1}$ as compared to 94 $m^2$ $g^{-1}$ found for ZnS). Increasing coverage changes the surface area in direction of the CdS value. Accordingly, the specific surface area of CdS-*x*/$SiO_2$ decreases from 280 to 250 and 233 to 188 $m^2$ $g^{-1}$, when the coverage increases from 4 to 11 and 17 to 25% (Table 1). Contrary to this, for the ZnS supported materials the specific surface area increases with increasing coverage, although very moderately as indicated by the values of 95 and 104 $m^2$ $g^{-1}$ measured for 5 and 30% coverage, respectively. This comparable weaker effect is in accord with the much smaller difference in surface areas between support and CdS than in the case of $SiO_2$. Sonication during sample preparation decreases the mean size of about the half of the particles from 55 to 25 μm (Fig. 2).

### CdS-*x*/$SiO_2$

Upon irradiation at $\lambda \geq 290$ nm the absolute product concentrations for the $SiO_2$ supported samples are in the range of 70–80 μM and differ only negligibly from the values obtained with unsupported CdS (Fig. 3). ZnS supported catalysts behave similarly, except for CdS-05/ZnS (*vide infra*).

As expected, the apparent turnover numbers $TON_{app}$ of supported cadmium sulfides are much higher than that of the unsupported sample (Fig. 3). Since silica induced the strongest effect, the dependence of product formation on coverage, catalyst concentration and pH value was investigated with the sample CdS-17/$SiO_2$. In addition to the two-electron reduction product formate, the four-electron product formaldehyde is formed in comparable concentrations of 15–35 μM whereas the $C_2$-product oxalate reaches only 1–8 μM. The formation of formate occurs most likely through a $2e^-$-process (−0.59 V) according to eqn. (1) since the potential of the conduction band electrons (−0.59 V) is not negative enough to allow a $1e^-$-reduction of $CO_2$ (−2.21 V, Fig. 7).

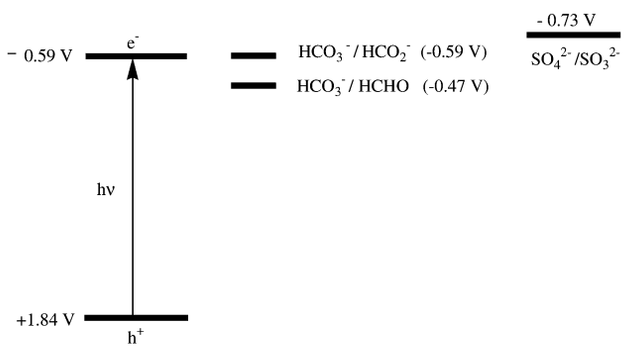


**Fig. 7** Band positions of CdS-17/$SiO_2$[9] and reduction potentials of $HCO_3^-$ at pH 7.[10]

$$HCO_3^- + 2e^- + 2H^+ \longrightarrow HCO_2^- + H_2O \qquad (1)$$

Formaldehyde is not formed *via* intermediate formate since only the known back-oxidation to $CO_2$, but no formaldehyde formation, is observed when bicarbonate is replaced by formate in the system CdS-17/$SiO_2$/$Na_2SO_3$–$NaHCO_3$. This assumption is also supported by the different dependence of formate and formaldehyde concentrations on coverage and catalyst concentration (Fig. 4 and 5). Contrary to the case of formaldehyde, oxalate is formed *via* intermediate formate through oxidation by valence band holes since in the system CdS-17/$SiO_2$/$Na_2SO_3$–$NaHCO_3$ replacement of sulfite by formate induces the formation of oxalate. This is in agreement with the increase of oxalate concentration to a constant high value whereas the formate concentration decreases to a constant low value upon increasing the catalyst concentration (Fig. 5). The linear increase of oxalate concentration with coverage (Fig. 4) can be rationalized under the assumption that dimerization of the $CO_2^-$ radical does not occur on the CdS surface but in solution or on the $SiO_2$ surface and that it competes with the further oxidation to $CO_2$. Thus, $CO_2^-$ produced according to eqn. (2) may inject an electron into the conduction band [eqn. (3)] or desorb into solution (or onto silica) and dimerize [eqn. (4) and (5a)]; dimerization may occur also between adsorbed and solvated radicals [eqn. (5b)]. With increasing coverage the area

of the CdS/solution interface should increase and therefore also the number of $CO_2^-$ radicals desorbing per unit area. Since the rate of dimerization increases quadratically with the radical concentration, dimerization should be more strongly favored than oxidation with increasing coverage [eqn. (3)].

$$HCO_2^-{}_{(ad)} + h^+ \longrightarrow H^+ + CO_2^-{}_{(ad)} \quad (2)$$

$$CO^-{}_{2(ad)} \longrightarrow CO_{2(solv)} + e^-{}_{cb} \quad (3)$$

$$CO_2^-{}_{(ad)} \longrightarrow CO_2^-{}_{(solv)} \quad (4)$$

$$2\,CO_2^-{}_{(solv)} \longrightarrow C_2O_4^{2-}{}_{(solv)} \quad (5a)$$

$$CO_2^-{}_{(solv)} + CO^-{}_{2(ad)} \longrightarrow C_2O_4^{2-}{}_{(solv)} \quad (5b)$$

Increasing the standard concentration of bicarbonate in the system CdS-17/$SiO_2$/$Na_2SO_3$–$NaHCO_3$ from 33 to 60 mM enhanced the formate production by 10%. A stronger influence was observed upon changing the proton concentration. When the pH value of the standard reaction, pH 8.1, was increased to 10.0 and 11.9, the formate concentration increased by 20 and 100%, respectively (Fig. 8). Contrary to this, the concentration

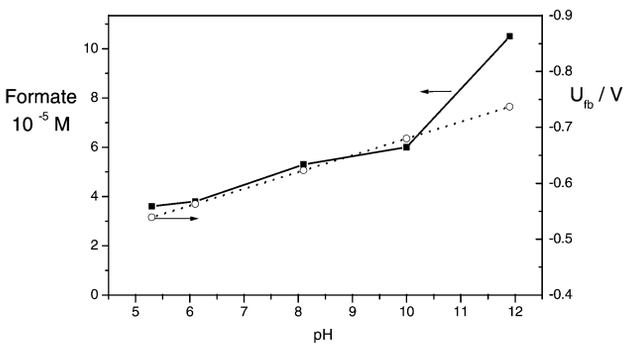


**Fig. 8** Dependence of formate formation and calculated flatband potential[9] on the pH value; CdS-17/$SiO_2$, $\lambda \geq 290$ nm, 6 h.

decreased by 20% when the pH value was lowered to 6.1 or 5.3. When sodium bicarbonate was replaced by sodium carbonate (33 mM), it resulted in a pH value of 11.2 and the formate concentration increased by 25%. This moderate increase of photocatalytic activity upon increasing the pH value from 8.1 to 10 and 11.9 suggests that it is caused by the moderate cathodic shift of the flatband potential from −0.62 to −0.69 and −0.73 V, respectively,[9] and not by the much stronger increase of carbonate concentration over two and four orders of magnitude. The resulting more negative potential of the conduction band electron should induce an easier reduction of bicarbonate [eqn. (1)].

The positive influence of the silica support on the reaction rate significantly depends on the irradiation wavelength. Compared to unsupported CdS the formate concentration after 5 h is 1.6 times higher at the shorter wavelengths (Fig. 9, A) whereas it is 6.0 times higher at longer wavelengths (Fig. 9, B). This significant dependence on the wavelength makes it unlikely that the support may induce a better substrate adsorption and thereby increases the efficiency of the IFET reactions. It rather suggests that the positive influence is due to an electronic semiconductor–support interaction (SEMSI) which increases the bandgap and therefore the driving force of the IFET.[9]

### CdS-*x*/ZnS

Since, contrary to the silica support, zinc sulfide is photoactive in the photoreduction of carbon dioxide,[5] irradiation conditions for CdS-*x*/ZnS were selected in order that only CdS

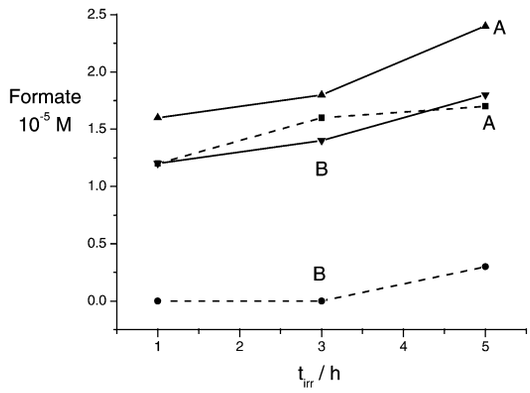


**Fig. 9** The influence of short (A: $\lambda \geq 320$ nm) and long (B: $\lambda \geq 455$ nm) wavelength irradiation for unsupported (---) and supported (——, CdS-17/$SiO_2$) cadmium sulfide.

($\lambda_{bg} \leq 536$ nm) or ZnS ($\lambda_{bg} \leq 336$ nm) could absorb the light. When the former is the case ($\lambda \geq 455$ nm), the photocatalytic activity is strongly enhanced compared to the unsupported CdS. Whereas bare CdS produces only traces of formate after 3 h irradiation time, the ZnS supported samples give rise to concentrations of 22–40 μM (Fig. 6). Similarly, as discussed for the silica support, this positive influence is assumed to be a consequence of a novel SEMSI effect.[9]

At irradiation conditions where both CdS and ZnS can absorb ($\lambda \geq 320$ nm), the difference in activity of CdS-*x*/ZnS, $x = 10$, 20, 30%, relative to unsupported CdS is rather moderate. Contrary to this, the sample with $x = 5$% induces a 40-fold and 16-fold increase compared to CdS and ZnS, respectively (Fig. 10). This exceptional difference between CdS-05/ZnS and

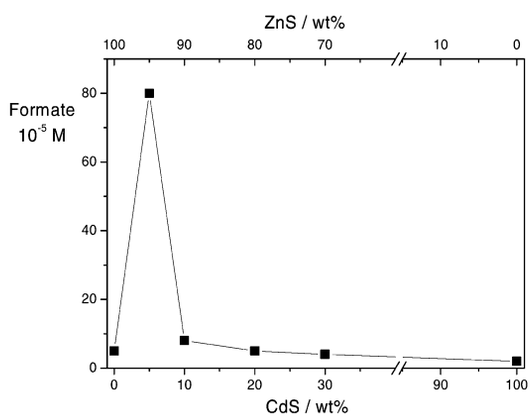


**Fig. 10** Relation between formate concentration and coverage for CdS-*x*/ZnS; $\lambda \geq 320$ nm, 3h.

CdS-10/ZnS may be rationalized by assuming that for the lower coverage light absorption by ZnS is much stronger than by CdS thus generating ZnS localized electron-hole pairs, from which electron injection into the conduction band of CdS may occur (Fig. 11). As a result recombination is inhibited and the

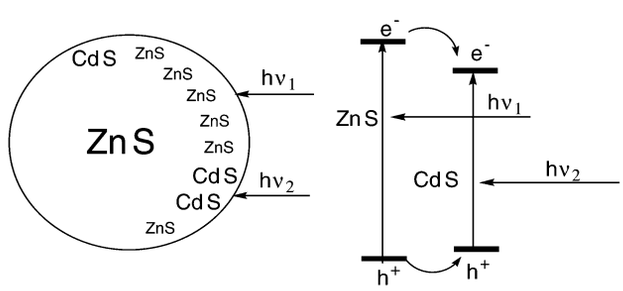


**Fig. 11** Schematic description of interparticle electron transfer at CdS-05/ZnS.

efficiency of charge separation is increased. A similar interparticle electron transfer was invoked for coupled CdS/$TiO_2$ systems to explain increased reaction rates.[1d,e,11]

This interpretation is supported by the strong dependence of photocatalytic activity on irradiation conditions. At $\lambda \geq 400$, 455 nm the formate concentration after 2 h was found to be only 2 μM, whereas it reached 130 μM at $\lambda \geq 320$ nm. The subsequent activity decrease is due to a complete consumption of sulfite as indicated by HPLC analysis.

Monochromatic experiments at 317 and 436 nm indicated that this acceleration of formate formation by CdS-05/$SiO_2$ is a true wavelength effect. Whereas after 20 h the product concentration reached 20 μM in the case of irradiation at the shorter wavelength, no formate was detectable when light of the longer wavelength was employed although its intensity was 35-fold higher. This may suggest that at the CdS component the IFET to $HCO_3^-$–$CO_3^{2-}$ occurs from surface states (hot electrons) located above the conduction band edge and that this is the rate-determining step. However, a more efficient charge-separation through the interparticle electron transfer may cause the same effect. The observation that increasing the standard sulfite concentration in the CdS-05/ZnS/$Na_2SO_3$–$NaHCO_3$ system from 0.005 M to 0.01 M does not change the initial rate of formate formation supports the postulate that the reductive IFET step determines the reaction rate.

## Summary

In conclusion, the results presented above demonstrate that both silica and zinc sulfide supports increase the photocatalytic activity of cadmium sulfide through the presence of an electronic semiconductor–support interaction (SEMSI effect). Additionally, the low coverage sample CdS-05/ZnS combines this novel effect with the higher charge separation efficiency of a coupled semiconductor system.

## References


1 (*a*) L. Spanhel, H. Weller and A. Henglein, Photochemistry of semiconductor colloids. Electron injection from illuminated CdS into attached $TiO_2$ and ZnO A, *J. Am. Chem. Soc.*, 1987, **109**, 6632; (*b*) S. Hotchandani and P. V. Kamat, Charge-transfer processes in coupled semiconductor systems. Photochemistry and photoelectrochemistry of the colloidal cadmium sulfide-zinc oxide system, *J. Phys. Chem. B.*, 1992, **96**, 6834; (*c*) N. Serpone, E. Borgarello and M. Grätzel, Visible light induced generation of hydrogen from $H_2S$ in mixed semiconductor dispersions; Improved efficiency through interparticle electron transfer, *J. Chem. Soc., Chem. Commun.*, 1984, 342; (*d*) K. R. Gopidas, M. Bohorquez and P. V. Kamat, Photophysical and photochemical aspects of coupled semiconductors: Charge transfer processes in colloidal cadmium sulfide-titania and cadmium sulfide-silver iodide systems, *J. Phys. Chem.*, 1990, **94**, 6435; (*e*) N. Serpone, P. Maruthamuthu, P. Pichat, E. Pelizzetti and H. Hidaka, Exploiting the interparticle electron transfer process in the photocatalyzed oxidation of phenol, 2-chlorophenol and pentachlorophenol: chemical evidence for electron and hole transfer between coupled semiconductors, *J. Photochem. Photobiol., A*, 1995, **85**, 247.

2 C. Anderson and A. J. Bard, Improved photocatalytic activity and characterization of mixed $TiO_2/SiO_2$ and $TiO_2/Al_2O_3$ materials, *J. Phys. Chem. B*, 1997, **101**, 2611.

3 (*a*) B. R. Eggins, J. T. S. Irvine, E. P. Murphy and J. Grimshaw, Formation of two-carbon acids from carbon dioxide by photoreduction on cadmium sulfide, *J. Chem. Soc., Chem. Commun.*, 1988, 1123; (*b*) M. M. Taqui Khan, S. B. Halligudi and S. Shukla, Stoichiometric reduction of carbon dioxide to HCHO and HCOOH by $K[Ru^{III}(EDTA\text{-}H)]Cl \times 2H_2O$, *J. Mol. Catal.*, 1989, **53**, 305; (*c*) J. T. S. Irvine, B. R. Eggins and J. Grimshaw, Solar energy fixation of carbon dioxide via cadmium sulfide and other semiconductor photocatalysis, *Sol. Energy*, 1990, **45**, 27; (*d*) B. R. Eggins, P. K. J. Robertson, E. P. Murphy, E. Woods and J. T. S. Irvine, Factors affecting the photoelectrochemical fixation of carbon dioxide with semiconductor colloids, *J. Photochem. Photobiol., A*, 1998, **118**, 31; (*e*) B.-J. Liu, T. Torimoto and H. Yoneyama, Photocatalytic reduction of $CO_2$ using surface-modified CdS photocatalysis in organic solvents, *J. Photochem. Photobiol, A*, 1998, **113**, 93; (*f*) H. Fujiwara, H. Hosokawa, K. Murakoshi, Y. Wada, Sh. Yanagida, T. Okada and H. Kobayashi, Effect of surface structures on photocatalytic $CO_2$ reduction using quantized CdS nanocrystallines, *J. Phys. Chem. B*, 1997, **101**, 8270; (*g*) Sh. Yanagida, M. Kanemoto, K.-I. Ishihara, Y. Wada, T. Sakata and H. Mori, Semiconductor photocatalysis. Part 22. Visible light induced photoreduction of $CO_2$ with CdS nanocrystallites – importance of the morphology and surface structures controlled through solvation by N,N-dimethylformamide, *Bull. Chem. Soc. Jpn.*, 1997, **70**, 2063; (*h*) H. Inoue, R. Nakamura and H. Yoneyama, Effect of charged conditions of stabilizers for cadmium sulfide microcrystalline photocatalysts on photoreduction of carbon dioxide, *Chem. Lett.*, 1994, 1227; (*i*) M. Kanemoto, M. Nomura, Y. Wada, T. Akano and S. Yanagida, Effect of $In^{3+}$ in nano-scale CdS-catalyzed photoreduction of $CO_2$, *Chem. Lett.*, 1993, 1687; (*j*) M. Kanemoto, K. Ishihara, Y. Wada, T. Sakata, H. Mori and S. Yanagida, Visible light induced effective photoreduction of $CO_2$ to CO catalyzed by colloidal CdS microcrystallites, *Chem. Lett.*, 1992, 835; (*k*) S. M. Aliwi and K. F. Al-Jubori, Photoreduction of carbon dioxide by metal sulfide semiconductors in presence of hydrogen sulfide, *Sol. Energy Mater.*, 1989, **18**, 223.

4 (*a*) Y. Wada, T. Kitamura and S. Yanagida, $CO_2$-fixation into organic carbonyl compounds in visible-light-induced photocatalysis of linear aromatic compounds, *Res. Chem. Intermed.*, 2000, **26**, 153; (*b*) M. Kanemoto, H. Ankyu, Y. Wada and S. Yanagida, Semiconductor photocatalysis. Part 14. Visible-light induced photofixation of carbon dioxide into benzophenone catalyzed by colloidal cadmium microcrystallites, *Chem. Lett.*, 1992, 2113; (*c*) H. Inoue, Y. Kubo and H. Yoneyama, Photocatalytic fixation of carbon dioxide in oxoglutaric acid using isocitrate dehydrogenase and cadmium sulfide, *J. Chem. Soc., Faraday Trans.*, 1991, **87**, 553.

5 P. Johne and H. Kisch, Photoreduction of carbon dioxide catalysed by free and supported zinc and cadmium sulfide powders, *J. Photochem. Photobiol., A*, 1997, **111**, 223.

6 W. M. Grant, Colorimetric microdetermination of formic acid based on reduction to formaldehyde, *Anal. Chem.*, 1948, **3**, 267.

7 A. Reinheimer, R. van Eldik and H. Kisch, On the mechanism of radical C-N coupling in type B semiconductor photocatalysis. A high-pressure study, *J. Phys. Chem. B*, 2000, **104**, 1014.

8 G. Hörner, P. Johne, R. Künneth, G. Twardzik and H. Kisch, Heterogeneous photocatalysis, Part XIX. Semiconductor type A photocatalysis: Role of substrate adsorbtion and the nature of photoreactive surface sites in zinc sulfide catalyzed C-C coupling reactions, *Chem. Eur. J.*, 1999, **5**, 208.

9 H. Weiß, A. Fernandez and H. Kisch, Electronic semiconductor-support interaction. A novel effect in semiconductor photocatalysis, *Angew. Chem.*, 2001, **113**, 3942 (*Angew. Chem., Int. Ed.*, 2001, **40**, 3825).

10 The standard potentials for the reduction of $H_2CO_3$ were converted to pH 7; A. J. Bard, R. Parsons and J. Jordan, *Standard Potentials in Aqueous Solution*, M. Decker, New York and Basel, 1985, p. 195.

11 Different from the present case, only the smaller bandgap semiconductor (CdS) absorbs the light in the system CdS/$TiO_2$, ref. 1*d* and *e*.